



Time resolved study of three ruthenium(II) complexes at micellar surfaces: A new long excited state lifetime probe for determining *critical micelle concentration* of surfactant nano-aggregates



Digambara Patra*, Ahmad H. Chaaban, Shaza Darwish, Huda A. Saad, Ali S. Nehme, Tarek H. Ghaddar*

Department of Chemistry, American University of Beirut, Beirut, Lebanon

ARTICLE INFO

Article history:

Received 13 August 2015

Received in revised form 24 October 2015

Accepted 19 November 2015

Available online 23 November 2015

Keywords:

Ruthenium complex

Luminescence

Excited state lifetime

Surfactant

cmc

ABSTRACT

Three different ruthenium complexes have been synthesized and their luminescence properties in different solvent environments are reported. Luminescence intensities and excited state lifetimes of **Ru-I**, **Ru-II** and **Ru-III** vary with solvent viscosity. The excited state lifetime of **Ru-I** linearly increases in the viscosity range 1.76–12,100 cP. **Ru-II** shows two linear increases: one in the low and another in the high viscosity ranges, whereas **Ru-III** illustrates a linear enhancement only in the low viscosity range. Interestingly, luminescence intensities and excited state lifetimes of **Ru-I**, **Ru-II** and **Ru-III** are found to be sensitive to nano-aggregation. However, the surfactant head charge and that of the ruthenium center as well as the hydrophobic tail of the ancillary ligand of the complexes have a great role in deciding the nature of the interaction and on the excited state properties at micellar surfaces. It is proposed that the long lifetime of **Ru-III** in water could be due to the coiling of the carbon chain of the ancillary ligand around the ruthenium center. At micelle surface, this coiling of the carbon chain is lost due to the parallel alignment with surfactants and thus quenching of the excited state lifetime is seen. Furthermore, it is shown that the variation of the excited state lifetime with respect to the change in surfactant concentration is a result of the formation of micelles from the surfactant monomer, thus, a novel technique for the determination of the *critical micelle concentration* (cmc) based on the long excited state lifetime of **Ru-III** located at the micellar nano-aggregates is reported.

© 2015 Elsevier B.V. All rights reserved.

1. Introduction

Transition metal complexes have drawn much interest because of their chemotherapeutic applications [1]. Ruthenium complexes have shown less general toxicity than platinum complexes [2–5], which sets them at the heart of research for various applications, in addition to their usage in solar cells [6–9]. Ruthenium(II) polypyridyl complexes have attracted significant interest due to their exciting photophysical and photochemical properties [10–15]. In a transition metal complex, one can broadly classify the electronic transitions into at least four different categories, though such approximation may not describe the electronic structures very well. These four transitions include (i) intra-ligand transition ($\pi_L-\pi_L^*$) which is similar to that of the free ligand, (ii) metal to ligand charge transfer, MLCT ($t_{2g}-\pi_L^*$), (iii) metal centred (MC) or dd transition ($t_{2g}-e_g$ orbitals), (iv) and ligand to metal charge trans-

fer (π_L-e_g). Other transitions include ligand to ligand and metal to metal charge transfers. The lowest excited state of a ruthenium complex is luminescent with a sufficiently long lifetime that could engage in photo-redox and photo-chemical reactions. Judiciously choosing the pH, solvent and the polypyridyl ligand, one can alter these properties [16–22]. Tuning the excited state properties of ruthenium complexes is central to defining their practical applications.

In our day-to-day life and in industry, surfactants have extensive uses in many consumer products. Surfactants are the powerhouse of detergents, toothpastes, cosmetics etc. The type of surfactant in use depends on the application, such as the removal of dirt and grease from fibers and surfaces and the conditioning of the former. Micellar solutions have immense applications in catalysis, drug delivery and material sciences [23–26], such as gold nanorod preparation [27] and multicomponent analysis of poly-aromatic heterocycles (PAHs) without a separation procedure [28,29].

In aqueous solution, micelles with concentrations above the *critical micelle concentration* (cmc) exhibit extraordinary physico-chemical properties as a result of surfactant nano-aggregation

* Corresponding authors. Fax: +9611365217.

E-mail addresses: dp03@aub.edu.lb (D. Patra), tg02@aub.edu.lb (T.H. Ghaddar).

[23,30]. Both the size and the shape of these surfactant aggregates are known to depend on a variety of factors such as surfactant and salt concentrations, temperature, pH, etc. [23]. *cmc* of surfactants can be either determined by simple techniques, such as osmotic pressure, ionic conductance, capillary electrophoresis, scattered light intensity and Hyper-Rayleigh Scattering [30], or by spectroscopic techniques, such as NMR and fluorescence. Fluorescence/luminescence methods appear to be more practical due to their simplicity, sensitivity, and fast execution; they also do not require special solvents such as the ones used in NMR. Among the numerous probe molecules that has been reported in the literature for *cmc* determination [31–34] pyrene is the most widely used one [31].

The change in fluorescence/luminescence intensity of a probe as a function of surfactant concentration determines the *cmc*. A break in the plot of fluorescence intensity versus concentration often signifies the formation of micellar aggregates. Knowing that the fluorescence/luminescence intensity is sensitive to the amount of the fluorophore/probe present in solution, the amount of the probe should be carefully controlled. On the other hand, the excited state lifetime is insensitive to the probe amount. Therefore finding a probe molecule that is sensitive to *cmc* formation based on its excited state lifetime is highly desirable. In this work, we have synthesized three different ruthenium(II) complexes as given in Scheme 1. The spectroscopic characterization of these three complexes, named as **Ru-I**, **Ru-II** and **Ru-III**, has been evaluated in various solvent environments. Luminescence properties of these complexes have been investigated in glycerol/water mixtures to understand the influence of solvent viscosity on the luminescence intensity, luminescence spectrum and excited state lifetime. Finally, the photophysical properties of these complexes, especially **Ru-II** and **Ru-III**, have been studied in five different cationic, anionic and neutral surfactant solutions. Not only the luminescence intensity of **Ru-III** was able to sense *cmc* of these surfactant solutions but also its excited state lifetime offered an alternative approach to estimate *cmc*. We, herein, propose a possible mechanism on how *cmc* can be inferred from the excited state lifetime of the **Ru-III** complex.

2. Experimental

2.1. Materials

For synthesis, all solvents, reagents and organic starting material were purchased from Sigma–Aldrich and used without further purification, unless otherwise stated. All metal complexes were purchased from Strem Chemicals Inc. (MA, USA). For spectroscopic measurements, the solvents used were of spectroscopic or HPLC grades. The surfactants, CTAB [hexadecyltrimethylammonium bromide, 99+%], SDS [dodecyl sulphate sodium salt, 98%] and TX100 [4-(1,1,3,3-tetramethylbutyl) phenyl–polyethylene glycol] were obtained from Sigma–Aldrich. HDPB [hexadecyl pyridinium bromide] and DBSA [dodecyl benzene sulphonic acid] were received from Acros. The surfactant solutions of different concentrations were prepared by dissolving the respective surfactant in different amounts of doubly distilled water. The stock solutions consisted of 10 mM CTAB, 10 mM HDPB, 100 mM SDS, 100 mM DBSA and 10 mM TX-100.

2.2. Synthesis of Ru-I, Ru-II and Ru-III

4-Dodecylsulfanylbenzaldehyde [35], **Ru-I** [36], 4,4'-distyryl-2,2'-bipyridine and 4,4'-bis-[2-(4-dodecylsulfanyl-phenyl)-vinyl]-2,2'-bipyridine [37] were prepared according to previously described procedures in the literature.

Preparation of Ru-II and Ru-III: *cis*-Dichloro-bis(2,2'-bipyridine) ruthenium(II) (Eq. (1)) and the corresponding bipyridine ligand (1 eq.) were dissolved in ethanol and 10% distilled water was added. The reaction mixture was refluxed under nitrogen for 24 h in the absence of light. After cooling, the solvent was evaporated under reduced pressure and the crude solid was dissolved in water/acetone. Upon stirring, ammonium hexafluoro phosphate in water was added and the resulting precipitate was filtered. The crude solid was purified by gel-filtration chromatography on a Sephadex LH-20 column.

Ru-II: $^1\text{H NMR}$ (d_6 -DMSO), δ (ppm): 7.38 (d, $J=17$ Hz, 2H), 7.43–7.58 (m, 6H), 7.65 (s, 2H), 7.70–7.84 (m, 16H), 7.86 (d, $J=17$ Hz, 2H), 8.17 (t, 2H), 8.82 (d, $J=8$ Hz, 4H), 9.08 (s, 2H). APPI MS (m/z): calculated for $\text{C}_{46}\text{H}_{36}\text{F}_6\text{N}_6\text{PRu}$ [$\text{M} - \text{PF}_6$] $^+$, 919.2; found, 918.6.

Ru-III: $^1\text{H NMR}$ (d_6 -DMSO), δ (ppm): $^1\text{H NMR}$ (d_6 -DMSO), δ (ppm): 0.82 (t, 6H), 1.21–1.37 (m, 36H), 1.40–1.64 (m, 4H), 2.89 (t, 4H), 7.30 (d, $J=16$ Hz, 2H), 7.40–7.55 (m, 6H), 7.70–7.80 (m, 14H), 7.80 (d, $J=16$ Hz, 2H), 8.17 (m, 4H), 8.80 (d, $J=8$ Hz, 4H), 9.05 (s, 2H). APPI MS (m/z): calculated for $\text{C}_{70}\text{H}_{84}\text{F}_6\text{N}_6\text{PRuS}_2$ [$\text{M} - \text{PF}_6$] $^+$, 1319.5; found, 1318.7.

2.3. Spectroscopic measurements

The absorption spectra in various solvents and in cationic CTAB/HDPB, anionic SDS/DBSA, and neutral TX-100 were recorded at room temperature using a JASCO V-570 UV–VIS–NIR spectrophotometer. Luminescence measurements were obtained on a JOBIN YVON Horiba Fluorolog 3 spectrofluorometer. The excitation and emission slits width were 5 nm. The excitation source was a 100 W Xenon lamp and the detector used was R-928 operating at a voltage of 950 V. The spectral data were collected using Fluorescence software and OriginPro 6.0 software was used for further data analysis. For excited state lifetime measurements the same instrument was used, wherein a diode laser with a 405 nm excitation wavelength was used for excitation.

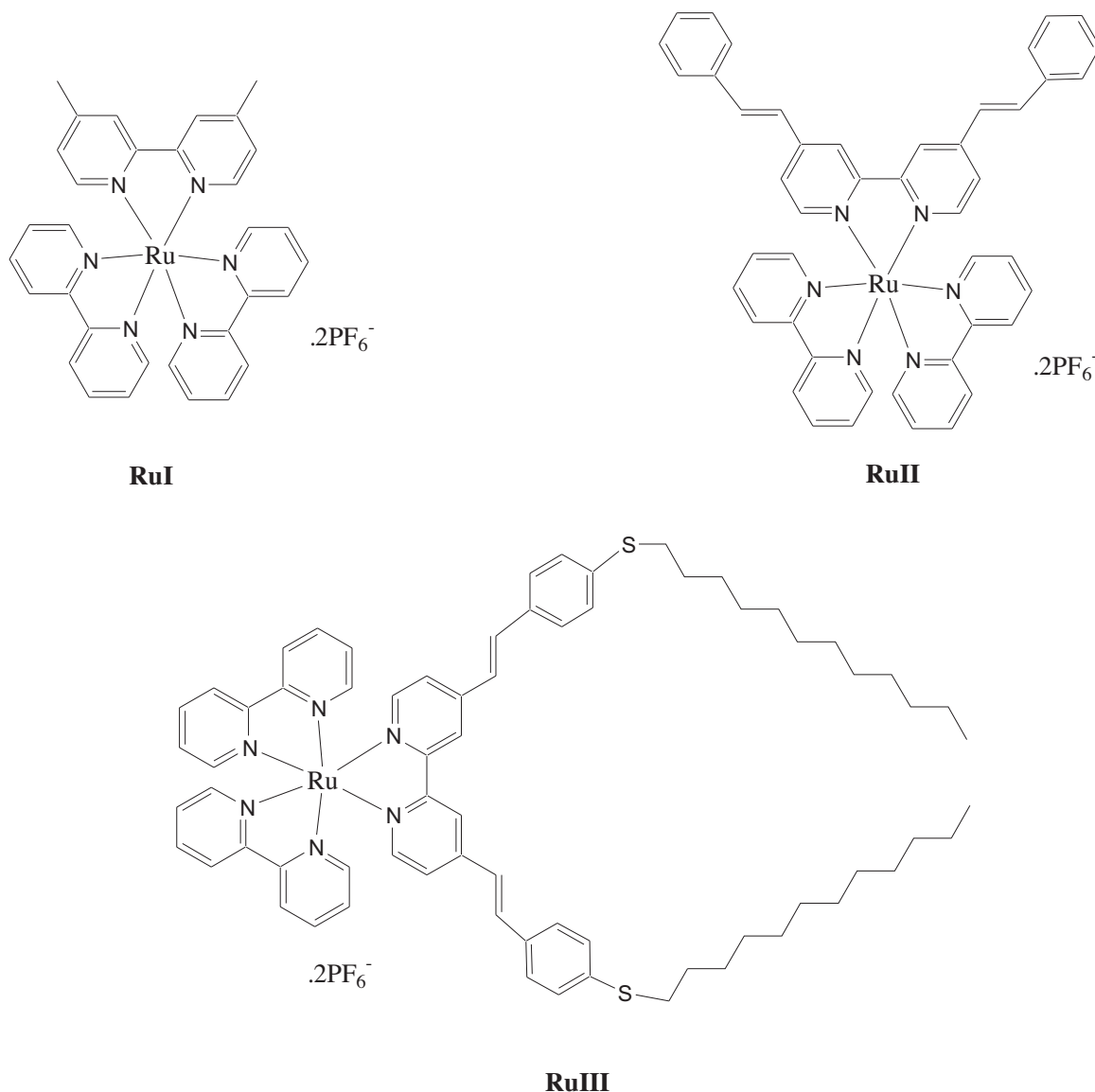
3. Results and discussion

3.1. Spectral properties

Among the various ruthenium polypyridyl complexes, $\text{Ru}(\text{bpy})_3^{2+}$ is most widely studied for its photophysical and excited state properties [38–45]. Since photophysical properties of $\text{Ru}(\text{bpy})_3^{2+}$ are relatively well understood, it is often used as a reference complex for comparing it with other Ru (II) polypyridyl complex. The visible absorption spectrum of $\text{Ru}(\text{bpy})_3^{2+}$ is related to a spin allowed metal-to-ligand charge transfer (MLCT) process where its excitation with light in the UV–visible regions leads to the well-known charge transfer phenomena from the lowest excited state [38–45].



$\text{Ru}(\text{bpy})_3^{2+}$ shows an absorption maximum at around 453 nm and an emission maximum at around 597 nm in water [46]. The lowest excited state of $\text{Ru}(\text{bpy})_3^{2+}$ is a triplet metal to ligand charge transfer state ($^3\text{MLCT}$) which is below the ^3MC and $^1\text{MLCT}$ excited states [47]. The lowest $^3\text{MLCT}$ is in fact a combination of closely lying three excited states that are at equilibrium at and above 77 K but distinguishable at 5 K [48,49]. However, a fourth $^3\text{MLCT}$ lies above these three lower energy states and is populated at temperatures above 200 K [47]. This fourth $^3\text{MLCT}$ state has considerably more singlet character than the other three lower lying $^3\text{MLCT}$ states, and thus makes the inter-system crossing and relaxation to the ground state by a non-radiative process more feasible. However, the photochem-



Scheme 1. Structure of **Ru-I**, **Ru-II** and **Ru-III**.

istry of $\text{Ru}(\text{bpy})_3^{2+}$ mainly arises from the ^3MC excited state. The ^3MC lies above the $^3\text{MLCT}$ and can be thermally populated from the latter. At the same time the ^3MC state is distorted with respect to the Ru–N bond distance compared with the $^3\text{MLCT}$ excited state and the ground state. The $^1\text{MLCT}$, ^1MC and $\pi_L-\pi_L^*$ transitions lie above the ^3MC . These transitions have been observed in electronic absorption spectra with absorption bands at 185 nm and 285 nm for $\pi_L-\pi^*$ transition and at 240 nm and 452 nm for $^1\text{MLCT}$ [50]. Regardless of their formal multiplicity, the excitation of $\text{Ru}(\text{bpy})_3^{2+}$ to all higher excited states is followed by fast internal conversion (IC) and inter-system crossing (ISC) to the lowest lying manifold of MLCT excited states with near unity efficiency [51]. It is noted that increasing the temperature above 77 K dramatically reduces luminescence quantum yield and emission lifetime which is due to the contribution of the solvent vibrational modes to the non-radiative decay of the $^3\text{MLCT}$.

In our present case, replacing one of the bipyridine ligand with a 4,4'-dimethyl-2,2'-bipyridine in **Ru-I** did not change the absorption maximum as shown in the excitation spectrum of **Ru-I** in Fig. S1 (see Supporting information), which showed a maximum at 453 nm. However, the emission maximum of **Ru-I** shifted slightly

to 614 nm in water with an additional band at ~ 660 nm. To enhance the hydrophobic nature of the ancillary ligand, the 4,4'-dimethyl-2,2'-bipyridine ligand was replaced with a phenylvinylene group in **Ru-II**. This modification did not change the absorption maximum but red shifted the emission maximum to 677 nm in **Ru-II** (see Fig. S2, S1). Furthermore, introducing a 12 carbon long chains in the *p*-position of the phenylvinylene groups as in **Ru-III** with a thioether linkage shifted the absorption maximum to 460 nm and the emission maximum to 680 nm, as shown in Fig. 1, indicating that the thioether linkage lowered the energy band gap of the MLCT band. The excited state lifetime of **Ru-I** showed a mono-exponential decay but the luminescence lifetime value was reduced from 580 ns to 322 ns when compared to $\text{Ru}(\text{bpy})_3^{2+}$ in water [52]. This lifetime was further reduced to 300 ns in the case of **Ru-II** in water. However, a biexponential decay was observed for **Ru-III**, where the longer component has a lifetime in the microsecond time scale and the calculated average excited state lifetime of **Ru-III** was remarkably enhanced by at least a 3.5 fold to a value of 1190 ns in water. This enhancement could be due to the introduction of the long carbon chains (the mechanism will be discussed at a later stage).

Table 1
Luminescence spectroscopic properties of **Ru-I**, **Ru-II** and **Ru-III** in various solvents.

Compound	Solvent	λ_{ex} (nm)	λ_{em} (nm)	τ (ns)	χ^2	Stokes shift
Ru (bpy) $^{2+}$	Water	453	600	580		
Ru-I	Methanol	452	603	224	1.06	5540
	Ethanol	451	605	227	0.94	5644
	Acetonitrile	451	608	151	0.91	5725
	DMSO	455	620	350	0.89	5848
	<i>n</i> -Butyronitrile	451	608	183	0.98	5726
	Chloroform	455	618	286	1.11	5797
Ru-II	Water	453	614	322	1.08	5788
	Methanol	450	644	97	1.07	6694
	Ethanol	460	639	83	0.87	6090
	Acetonitrile	442	661	87	1.10	7496
	DMSO	461	674	414	1.03	6855
	<i>n</i> -Butyronitrile	452	661	98	0.89	6995
Ru-III	Chloroform	455	663	72	1.62	6895
	Water	453	677	300	1.39	7304
	Methanol	456	668	93	0.81	6960
	Ethanol	460	669	112	1.01	6791
	Acetonitrile	457	671	100	0.78	6979
	DMSO	460	679	393	1.12	7012
	<i>n</i> -Butyronitrile	452	669	125	0.94	7176
	Chloroform	460	670	115	1.19	6814
Water	460	680	339 (17%) 1364(83%) ($\tau_{\text{av.}}$ = 1190 ns)	1.23	7033	

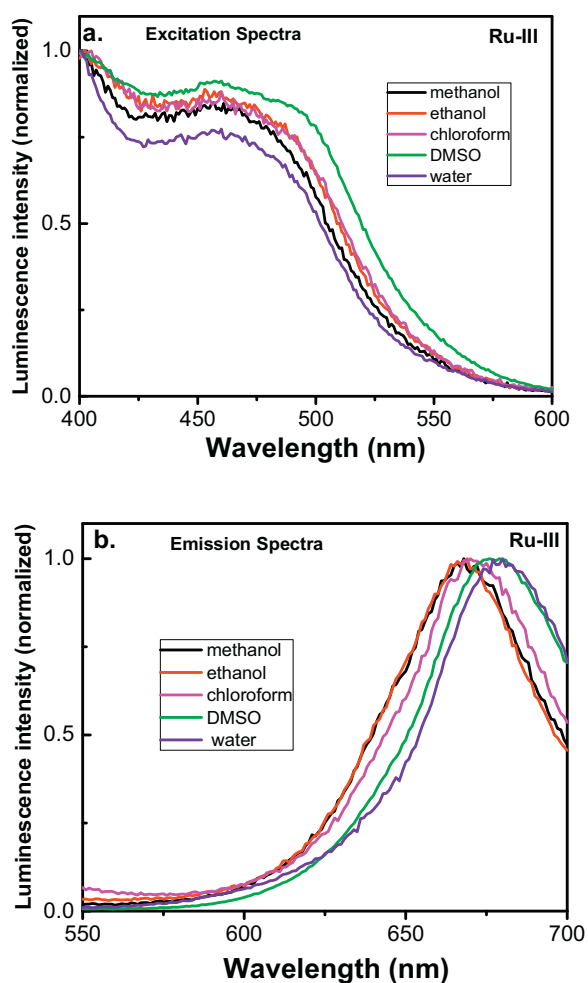


Fig. 1. Luminescence excitation and emission spectra of **Ru-III** in different solvents. The excitation spectrum was recorded at emission wavelength 680 nm and emission spectrum was recorded at excitation wavelength 433 nm.

3.2. Effect of solvent

Generally, solvents with different polarities always influence the luminescence properties of most fluorescence probes. As seen in Fig. 1 (see Figs. S2&S3, SI; data given in Table 1), the excitation and emission spectra of **Ru-I**, **Ru-II** and **Ru-III** were influenced by changing the solvent environment irrespective of the type of ruthenium complex. A red shift in the excitation and emission maxima in water and DMSO compared to methanol/acetonitrile was seen. The excited state lifetimes were also found to be longer in water and DMSO and fitted best to a mono-exponential decay. However, the fluorescence decay profile of **Ru-III** in water could be best fitted by a bi-exponential decay as mentioned above. The bi-exponential decay could be due to two separate interactions of **Ru-III** in water; where the positive charge head group would interact favorably with polar solvents and hence increases the excited state lifetime. In addition, the long carbon chain present in **Ru-III** would encourage a monolayer formation due to the hydrophobic nature and mismatch with the solvent molecules and affect the excited state lifetime. Stokes shift of **Ru-I** was found to be smaller than that of **Ru-II** and **Ru-III**, but there was no appreciable change in Stokes shift with respect to change in polarizability (Δf) and E_T (30) [34] (as given in Fig. S3, SI), suggesting that this complex may not be useful to investigate the polarity of the solvent medium.

To understand the effect of solvent viscosity on the luminescence behavior, glycerol was added to aqueous solutions in different proportions, thus, the viscosity of the solution was increased from 1.76 cP to 12,100 cP. The luminescence spectra of **Ru-I** (Fig. S4a, SI) and **Ru-II** (Fig. S4c, SI) did not change remarkably upon increasing the glycerol concentration, however, **Ru-III** (Fig. S4e, SI) showed a blue shift of about 5–6 nm in glycerol mixtures, which could be due to a specific interaction between the solute (**Ru-III**) and the solvent (water), solvent and co-solvent (glycerol) and/or solute and co-solvent. Since the effect of solvent polarity on the spectral properties of **Ru-I**, **Ru-II** and **Ru-III** was minimal; the spectral shift in the case of **Ru-III** could be more due to some interactions with glycerol. This is further evident from the fact that the luminescence intensity of **Ru-I** (Fig. S4b, SI), **Ru-II** (Fig. S4d, SI) and **Ru-III** (Fig. S4f, SI) consistently increased with the increase in viscosity, however, the increase was remarkably higher for **Ru-I**

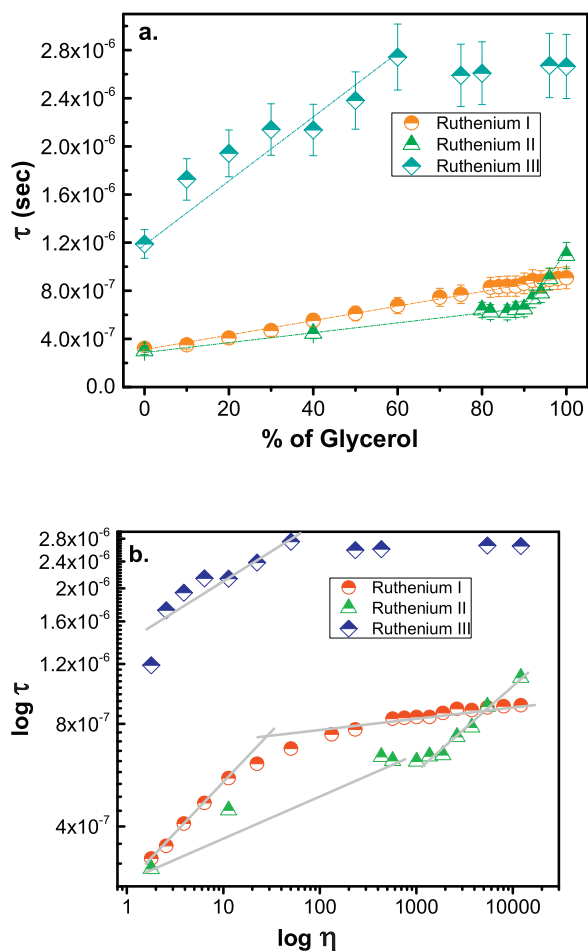


Fig. 2. (a) Plot of excited state lifetime of **Ru-I**, **Ru-II** and **Ru-III** vs. percentage of glycerol, error bars are given in SD ($n = 3$); (b) plot of $\log \tau$ vs. $\log \eta$.

and **Ru-II** when compared to **Ru-III**. The excited state lifetime of **Ru-I** increased consistently with increasing viscosity from 1.76 cP to 12,100 cP, but that of **Ru-II** and **Ru-III** gave two breaking points as provided in Fig. 2a. The lifetime values increased substantially at and above 90% glycerol for **Ru-II** whereas at and above 60% glycerol the excited state lifetime of **Ru-III** remained almost unchanged. The qualitative relationship between fluorescence parameters, such as lifetime (τ) of a molecule and the viscosity (η) of the immediate environment, is expressed by the Forster–Hoffmann equation [53] as

$$\log \tau = m \log \eta + C \quad (2)$$

where C is a term reflecting relaxation rate and temperature, and m is a molecule and temperature dependent constant. Under our measurement conditions in the aqueous glycerol mixtures (0–100%) we did not find a good linear fit (see Fig. 2b) for the whole viscosity range for any of the ruthenium complexes under investigation that fits well in a viscosity range lower than 100 cP.

3.3. Effect of surfactant solution

For potential biological applications the photophysical properties under physiological conditions are crucial. In order to mimic a biological membrane, the photophysical properties of **Ru-I**, **Ru-II** and **Ru-III** were investigated in neutral, cationic and anionic surfactant solutions, below and above the cmc . The interface of micelle–water is different from the bulk aqueous phase in many aspects. The micelle–water interface has many interesting proper-

ties; increased solubilisation of hydrophobic drug molecules is of particular interest. The size of such micelle aggregation has been found to be ~ 5 nm in diameter [54] and is influenced by various parameters. The nano-aggregation of a micelle is mostly due to electrostatic and hydrophobic interactions and thus, depending on the structure, probe molecules can be solubilized at a number of different sites. For this purpose five different surfactant solutions, two cationic surfactants, two anionic surfactants and a neutral one, were investigated using **Ru-I**, **Ru-II** and **Ru-III**.

3.4. Effect of cationic surfactant solution

The effect of cationic surfactant solutions on the luminescence spectra of the ruthenium complexes was studied. The luminescence spectra of **Ru-I** in CTAB did not change in its position and shape as reflected in Fig. S5a (Supporting information), where the luminescence intensity varied marginally till the cmc and afterwards remained more or less unchanged (see Fig. S5b, SI). The luminescence alteration of **Ru-I** in CTAB compared to aqueous solution confirms microencapsulation of the ruthenium complex into the micellar medium. Generally speaking, the excited state properties of ruthenium (II) complexes are not expected to be significantly affected in the presence of the cationic CTAB surfactant since the Coulombic repulsion between the cationic head group of CTAB and the positive charge of ruthenium (II) will force the complex to remain in the aqueous phase. This was further supported by the fact that there was no remarkable change in the excited state lifetime of **Ru-I** in CTAB surfactant solutions when compared to aqueous solution (see Fig. 3a and d). Interestingly, based on luminescence intensity change, a break point was observed around the cmc (see Fig. S5b, SI); the cmc of CTAB using luminescence intensity measurements is given in Table 2. Using **Ru-I**, the cmc of CTAB was estimated to be around 0.07 mM (breaking point), which is much lower than the one quantified by conductivity measurements [55] and the value reported in the literature [56]. It should be noted here that the value from conductivity measurements has been found to be slightly higher than the ones quantified by other methods reported in literature. Similarly, the luminescence intensity of **Ru-II** consistently increased with CTAB concentration without any change in luminescence spectral position. However, after the cmc point the luminescence intensity increased slowly for **Ru-II** (see Fig. S5c&d, SI). The obtained cmc using **Ru-II** as a probe was 0.09 mM. The excited state lifetime of **Ru-II**, as shown in Fig. 3b, was quenched in CTAB surfactant solution when compared to the aqueous solution, but the lifetime value almost remained independent of the CTAB concentration (see Fig. 3d). This suggests that the introduction of the phenylvinylene group in **Ru-II** somehow overcomes the unfavorable Coulombic repulsion between the ruthenium (II) center and the CTAB head groups. Interestingly, the trend in the spectral position changed as soon as long alkyl chains were introduced in the ancillary ligand as in **Ru-III**. Luminescence spectra of **Ru-III** (see Fig. S5e, SI) red shifted when going from water to CTAB surfactant solution, which is attributed to a strong hydrophobic interaction between the alkyl chains of the ligand in **Ru-III** and the alkyl chain of CTAB that overcomes any unfavorable Coulombic repulsions between the head groups of **Ru-III** and CTAB. The induced dipole moment within the complex upon the MLCT excitation reorients or displaces to the most favorable orientation on the CTAB micelles during the excited state lifetime. The change in luminescence intensity was dramatic with the addition of CTAB until the cmc was attained (see Fig. S5f, SI). The estimated cmc based on luminescence intensity change of **Ru-III** was found to be 0.26 mM, which is the same as the reported value in the literature [56] (refer to Table 2). Similarly, the excited state lifetime of **Ru-III** was quenched by CTAB as depicted in Fig. 3c, and it decreased until the cmc was reached, but at high post micelle concentration the life-

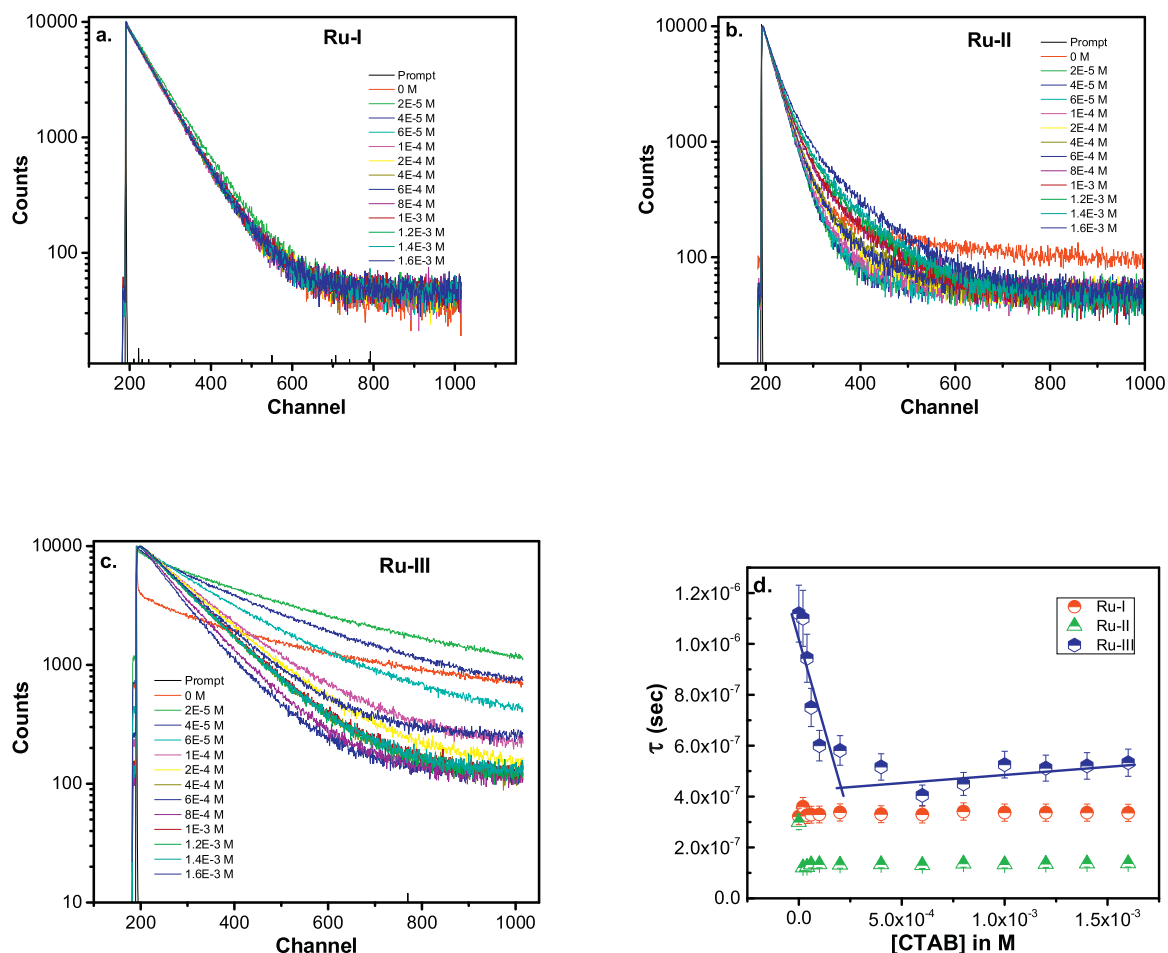


Fig. 3. Luminescence decay profile of **Ru-I** (a), **Ru-II** (b) and **Ru-III** (c) in CTAB surfactant solution. The excitation wavelength used was 405 nm. Luminescence was collected at 614 nm for **Ru-I**, at 677 nm for **Ru-II** and at 680 nm for **Ru-III**. (d) Plot of excited state lifetime (τ) vs. CTAB concentration for **Ru-I**, **Ru-II** and **Ru-III**, error bars are given in SD ($n=3$).

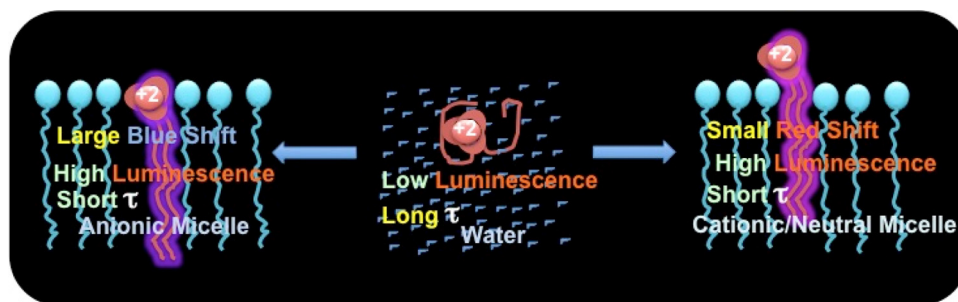
Table 2

Obtained *cmc* from luminescence intensity and excited state lifetime measurements.

Surfactant	Cmc values in mM							Literature values [56–58]
	Luminescence intensity measurement			Excited state lifetime measurement			Conductivity measurement [55,59]	
	Ru-I	Ru-II	Ru-III	Ru-I	Ru-II	Ru-III		
CTAB	0.07	0.09	0.26	ND	ND	0.21	0.98	0.26
SDS	NM	7.1	7.1	ND	2.1	7.0	8.0	6.0–8.0
HDPB	NM	ND	0.2	NM	ND	0.19	0.96	0.91
DBSA	NM	2.67	2.6	NM	ND	2.2	1.2	1.6
TX100	NM	0.11	0.15	NM	ND	0.11	0.29	0.9

NM: Not measured due to poor response of the probe.

ND: Not detected despite measurement was carried out.



Scheme 2. Illustration of alignment of **Ru-III** in aqueous phase, anionic micelle and cationic/neutral micelle along with their luminescence properties.

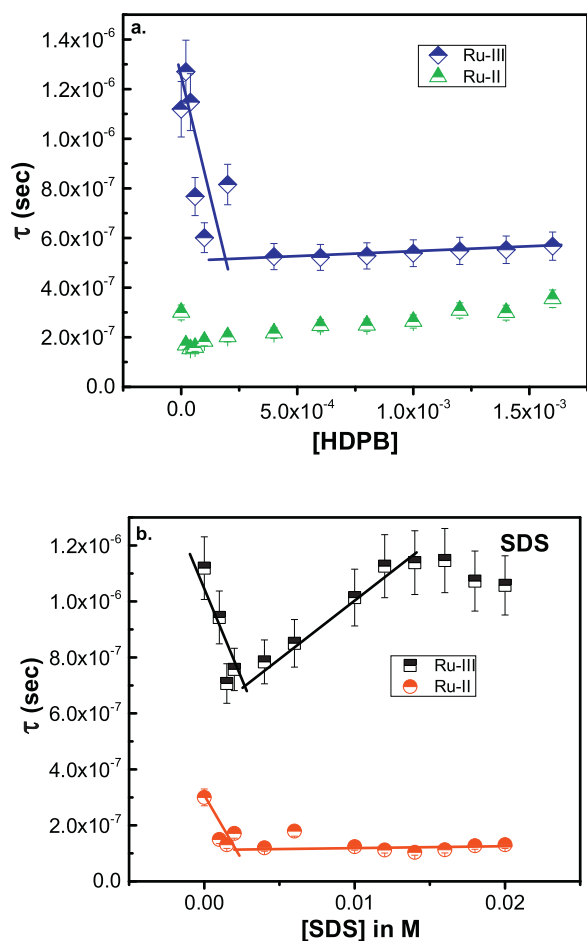


Fig. 4. (a) Plot of excited state lifetime (τ) vs. HDPB concentration for **Ru-II** and **Ru-III**; (b) Plot of excited state lifetime (τ) vs. SDS concentration for **Ru-II** and **Ru-III**. Error bars are given in SD ($n = 3$).

time remained unchanged. The variation in lifetime gave a breaking point at cmc (see Fig. 3d) and the cmc estimated for CTAB using excited state lifetime of **Ru-III** was as per the reported value [56] (see Table 2). The difference in cmc value obtained from luminescence intensity and excited state lifetime measurements of **Ru-III** is within the error margin. We propose that the hydrophobic tail of **Ru-III** plays a significant role in altering the excited state properties of the ruthenium center. The long lifetime of **Ru-III** could be due to coiling of the carbon chain around the ruthenium center and ligands (see Scheme 2). In a micelle, this coiling of chain is lost and the long chain aligns along with the surfactant (as shown in Scheme 2) thus causing quenching of the fluorescence lifetime of **Ru-III**. This is also true for the short component of the excited state lifetime in non-polar solvent. Among the three ruthenium complexes, the luminescence intensity of **Ru-I** was the least sensitive to aggregation of surfactants. Similarly, the excited state lifetime of **Ru-I** did not show any change before and after micelles were formed, which could be due to its relatively less hydrophobic nature. Since the excited state properties of **Ru-I** did not show sensitivity upon micellization, further studies in anionic and neutral surfactants or micellar media for **Ru-II** and **Ru-III** were chosen. When another cationic surfactant (HDPB) was used, the results obtained for **Ru-II** and **Ru-III** were similar to that obtained in the presence of CTAB. The cmc value obtained from luminescence intensity (shown in Fig. S6, SI) and excited state lifetime (see Fig. 4a) was comparable with the reported value in the literature [57] (Table 2).

3.5. Effect of anionic surfactant solution

The luminescence spectrum of **Ru-II** in SDS surfactant solution is depicted in Fig. S7a (Supporting information). The emission spectrum of **Ru-II** initially had a remarkable (more than 40 nm) blue shift with an equally appreciable enhancement in luminescence intensity upon going from an aqueous medium to the SDS surfactant solution. Indeed the emission spectrum showed a new band at ~ 630 nm which became the new emission maximum. Such a blue shift in the luminescence spectrum is due to the alteration of the medium from the aqueous phase to SDS surfactant pre-aggregates and micellar formation, which is favoured due to the attraction forces between the positive charge on the ruthenium (II) center and the negative charge of SDS. However, as the surfactant concentration further increased to higher concentrations, especially after the cmc , the emission spectrum shifted back to the red (to the original emission maximum) with a decrease in the luminescence intensity at ~ 630 nm. This shifting back of the emission spectrum suggests that the new band at ~ 630 nm is a result of strong Columbic attraction forces between the positive charges of the ruthenium(II) center and the negative head group of the surfactant molecule. With increase in the SDS concentration, hydrophobic interactions of SDS dominates by encouraging a micelle formation, thus, the strong monomer interaction between SDS and ruthenium(II) due to Columbic interactions subsidizes. This is further supported by the fact that the luminescence intensity of **Ru-II** increased until the cmc then decreased as shown in Fig. S7b (Supporting information). Therefore, the initial increase in luminescence intensity at lower concentration (below cmc) of SDS is ascribed to the progressive formation of pre-micellar aggregates, but as soon as a micelle is formed, the excited state of the ruthenium is quenched (see luminescence decay profile in Fig. S8a). The excited state lifetime also showed a similar behavior, where it was quenched marginally till the cmc and after wards remained unchanged (see Fig. 4b), especially at around the cmc where the lifetime value gave a quite unstable trend by introducing a high level of inaccuracy in cmc estimation. Therefore, the cmc obtained from the excited state lifetime measurement is much smaller than the one obtained from the luminescence intensity measurement of **Ru-II**. For **Ru-III**, the luminescence spectrum in SDS surfactant solution (given in Fig. S7c, SI) showed a remarkable blue shift compared to that in water. In this case the luminescence intensity increased until the cmc and afterwards it decreased as depicted in Fig. S7d (Supporting information). The blue shift in the case of **Ru-III** suggests that not only the Columbic interactions between the positively charged center of **Ru-III** and the negatively charged head group of SDS surfactant in addition to the hydrophobic interactions between the tail of **Ru-III** and the tail of the surfactant are facilitated. The cause of the appreciable blue shift in the spectrum is due to strong hydrophobic interactions that encourage the probe molecule to get buried easily into the surfactant structure and align itself parallel with the surfactant molecules. However, variation of the excited state decay profile (see Fig. S8b) and lifetime (Fig. 4b) of **Ru-III** with SDS concentration was found to be complex. This is understood because of the fact that the initial quenching of lifetime is favored by both Columbic attraction forces and hydrophobic interactions among individual SDS surfactant molecules and **Ru-III**. Later on when the micelle forms, more and more surfactant molecules join the nano-aggregation process, and therefore **Ru-III** acts as a stabilizer with the head groups of the surfactant molecules. This process exposes the ruthenium center to the aqueous phase despite the hydrophobic tail that is buried inside the core of the micelle (see Scheme 2). The cmc estimated by both luminescence intensity and excited state lifetime of **Ru-III** correlates well with the literature value [54] and within the marginal error. The results obtained for the

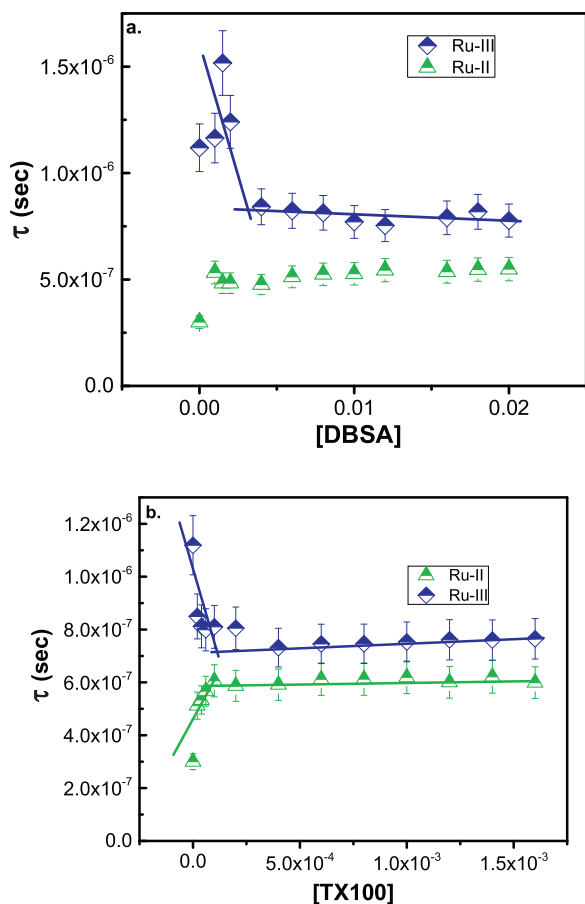


Fig. 5. (a) Plot of excited state lifetime (τ) vs. DBSA concentration for **Ru-II** and **Ru-III**; (b) Plot of excited state lifetime (τ) vs. TX100 concentration for **Ru-II** and **Ru-III**. Error bars are given in SD ($n=3$).

anionic surfactant, DBSA, were similar (given in Fig. 5a) and the obtained *cmc* value is similar to the reported one in literature [58] (see Table 2).

3.6. Effect of neutral surfactant solution

The luminescence spectra of **Ru-II** and **Ru-III** were investigated in the neutral Triton X-100 surfactant (TX100) and are provided in Fig. S9a&c (Supporting information). In both cases, the luminescence spectra showed red shifts in TX100 when compared to water. The luminescence intensities of **Ru-II** and **Ru-III** increased until the *cmc* was attained and remained constant post *cmc* (see Fig. S9b&d, SI). Similarly, the excited state lifetime profile (see Fig. S10a) of **Ru-II** increased slightly until *cmc* is reached and remained constant as shown in Fig. 5b. This could be attributed to the coiling of the neutral surfactant chain around the ruthenium complex which increases the excited state lifetime, similar to the earlier proposed case for **Ru-III** in water. However, the variation of the excited state lifetime profile (see Fig. S10b) of **Ru-III** was similar to that observed in CTAB surfactant solution (see Fig. 5b). The *cmc* obtained in TX100 using **Ru-III** excited state lifetime variation is similar to the reported one in the literature [56,59] and is given in Table 2.

4. Conclusion

Three different ruthenium complexes were successfully studied in various micellar solutions. The luminescence properties of these three complexes in different solvent environments did not show appreciable solvatochromic effects, but luminescence inten-

sity and excited state lifetimes of **Ru-I**, **Ru-II** and **Ru-III** were altered with varying the viscosity of the solvent. The excited state lifetime of **Ru-I** linearly increased in the viscosity range 1.76–12, 100 cP. **Ru-II** gave two linear rises: one corresponding to low and another to high viscosity ranges, whereas **Ru-III** showed a linear enhancement only in low viscosity ranges. The luminescence intensities of **Ru-II** and **Ru-III** were found to be sensitive to nano-aggregation. However, the charge on the head of the surfactant molecule and the ruthenium center as well as hydrophobic interactions concluded the nature of the excited state properties. The luminescence studies of **Ru-I**, **Ru-II** and **Ru-III** discussed here demonstrate that **Ru-III** can be advantageously applied as an excited state lifetime probe molecule for the determination of *cmc* of surfactant solutions. Thus, a novel technique for the determination of *cmc* based on the measurement of the excited state lifetime of **Ru-III** located at the micellar aggregate is reported. We conclude that the long lifetime of **Ru-III** in water is due to coiling of the carbon chain of the ligand around the ruthenium(II) center, however, in micellar solutions (or organic solvents) this coiling of the carbon chain is lost due to parallel alignment of the alkyl chains along with the surfactant's and thus quenching of the excited state lifetime is seen.

Acknowledgement

Financial support provided by American University of Beirut, Lebanon through URB, Kamal A. Shair Research Fund as well as Kamal A. Shair Central Research Science Laboratory (KAS CRSL) facilities to carry out this work is greatly acknowledged.

Appendix A. Supplementary data

Supplementary data associated with this article can be found, in the online version, at <http://dx.doi.org/10.1016/j.colsurfb.2015.11.037>.

References

- [1] L. Ronconi, P.J. Sadler, Using coordination chemistry to design new medicines, *Coord. Chem. Rev.* 251 (2007) 1633–1648.
- [2] A.R. Timerbaev, C.G. Hartinger, S.S. Aleksenko, B.K. Keppler, Interactions of antitumor metallodrugs with serum proteins: advances in characterization using modern analytical methodology, *Chem. Rev.* 106 (2006) 2224–2248.
- [3] C. Mari, V. Pierroz, S. Ferrari, G. Gasser, Combination of Ru (II) complexes and light: New Frontiers in cancer therapy, *Chem. Sci.* 6 (2015) 2660–2686.
- [4] F. Wang, J. Xu, A. Habtemariam, J. Bella, P.J. Sadler, Competition between glutathione and guanine for a ruthenium(II) arene anticancer complex: detection of a sulfenato intermediate, *J. Am. Chem. Soc.* 127 (2005) 17734–17743.
- [5] Z.-F. Chen, Q.-P. Qin, J.-L. Qin, J. Zhou, Y.-L. Li, N. Li, Y.-C. Liu, H. Liang, Water-soluble ruthenium(II) complexes with chiral 4-(2,3-dihydroxypropyl)-formamide oxoaporphine (FOA): in vitro and in vivo anticancer activity by stabilization of G-quadruplex DNA, inhibition of telomerase activity, and induction of tumor cell apoptosis, *J. Med. Chem.* 58 (2015) 4771–4789.
- [6] H. Kisserwan, A. Kamar, T. Shoker, T.H. Ghaddar, Photophysical properties of new cyclometalated ruthenium complexes and their use in dye sensitized solar cells, *Dalton Trans.* 41 (2012) 10643–10651.
- [7] H. Kisserwan, T.H. Ghaddar, Enhancement of photocurrent in dye sensitized solar cells incorporating a cyclometalated ruthenium complex with cuprous iodide as an electrolyte additive, *Dalton Trans.* 40 (2011) 3877–3884.
- [8] T.A. Shoker, T.H. Ghaddar, Novel poly-pyridyl ruthenium complexes with bis- and tris-tetrazolate mono-dentate ligands for dye sensitized solar cells, *RSC Adv.* 4 (2014) 18336–18340.
- [9] Y. Kageshima, H. Kumagai, T. Minegishi, J. Kubota, K. Domen, A photoelectrochemical solar cell consisting of a cadmium sulfide photoanode and a ruthenium-2,2'-bipyridine redox shuttle in a non-aqueous electrolyte, *Angew. Chem. Int. Ed.* 54 (2015) 7877–7881.
- [10] M.W. Mara, K.A. Fransted, L.X. Chen, Interplays of excited state structures and dynamics in copper(I) diimine complexes: implications and perspectives, *Coord. Chem. Rev.* 282–283 (2015) 2–18.
- [11] J.G. Wang, Y.L. Shang, Synthesis and photophysical and electrochemical properties of three novel Ru(II) complexes, *Mater. Res. Innov.* 17 (2013) 58–61.

- [12] Q.-H. Wei, Y.-F. Lei, W.-R. Xu, J.-M. Xie, G.-N. Chen, Ru(II) sensitized lanthanide luminescence: synthesis, photophysical properties, and near-infrared luminescence determination of alpha-fetal protein (AFP), *Dalton Trans.* 41 (2012) 11219–11225.
- [13] A. Sharmin, R.C. Darlington, K.I. Hardcastle, M. Ravera, E. Rosenberg, J.B. Alexander Ross, Tuning photophysical properties with ancillary ligands in Ru(II) mono-diimine complexes, *J. Organometal. Chem.* 694 (2009) 988–1000.
- [14] D.S. Tyson, K.B. Henbest, J. Bialecki, F.N. Castellano, Excited state processes in ruthenium(II)/pyrenyl complexes displaying extended lifetimes, *J. Phys. Chem. A* 105 (2001) 8154–8161.
- [15] D.J. Stufkens, A. Vlček Jr., Ligand-dependent excited state behaviour of Re(I) and Ru(II) carbonyl-diimine complexes, *Coord. Chem. Rev.* 177 (1998) 127–179.
- [16] A.S. Guerrero-Martínez, Y. Vida, D. Domínguez-Gutiérrez, R.Q. Albuquerque, L. De Cola, Turning emission properties of iridium and ruthenium meta; surfactants in micellar systems, *Inorg. Chem.* 47 (2008) 9131–9133.
- [17] S.K. Das, P.K. Dutta, Intrazeolitic photoreactions of Ru(bpy)₂²⁺ with methyl viologen, *Langmuir* 14 (1998) 5121–5126.
- [18] M.R. Arkin, E.D.A. Stemp, C. Turro, J.K. Barton, Luminescence quenching in supramolecular systems: a comparison of DNA- and SDS micelle-mediated photoinduced electron transfer between metal complexes, *J. Am. Chem. Soc.* 118 (1996) 2267–2274.
- [19] M. Szykora, J.R. Kincaid, P.K. Dutta, N.B. Castagnola, On the nature and extent of intermolecular interactions between entrapped complexes of Ru (bpy)₃²⁺ in zeolite Y, *J. Phys. Chem. B* 103 (1998) 309–320.
- [20] K. Matsui, K. Sasaki, N. Takahashi, Luminescence of tris(2,2'-bipyridine) ruthenium(II) in sol-gel glasses, *Langmuir* 7 (1991) 2866–2868.
- [21] S. Rajagopal, G.A. Gnananaraj, A. Mathew, C. Srinivasan, Excited state electron transfer reaction of tris(4,4'-dialkyl-2,2'-bipyridine) ruthenium(II) complexes with phenolate ions: structural and solvent effects, *J. Photochem. Photobiol. A* 69 (1992) 83–89.
- [22] E. Rajkumar, P.M. Mareeswaran, S. Rajagopal, Photophysical properties of amphiphilic ruthenium(II) complexes in micelles, *Photochem. Photobiol. Sci.* 13 (2014) 1261–1269.
- [23] J.H. Fendler, Membrane mimetic chemistry: characterization and applications of micelles, microemulsions, in: *Monolayers, Vesicles and Host-Guest Systems*, Wiley, New York, 1983.
- [24] D. Attwood, A.T. Florence, *Surfactant Systems: Their Chemistry, Pharmacy and Biology*, Chapman and Hall, London, 1983.
- [25] M.J. Rosen, *Surfactants and Interfacial Phenomena*, John Wiley & Sons, New Jersey, 2004.
- [26] R.J. Hunter, *Foundations of Colloid Science*, Oxford University Press, New York, 1991, Chapter 10.
- [27] R.N. Moussawi, D. Patra, Synthesis of Au nanorods through pre-reduction with curcumin: preferential enhancement of Au nanorods formation prepared from CTAB capped over citrate capped Au seeds, *J. Phys. Chem. C* 119 (2015) 19458–19468.
- [28] D. Patra, Simple luminescence method for estimation of benzo[a]pyrene in a complex mixture of polycyclic aromatic hydrocarbons without a pre-separation procedure, *Luminescence* 18 (2003) 97–102.
- [29] D. Patra, A.K. Mishra, Multivariate fluorimetric determination of mixture pyrene, perylene and triphenylene in water sample, *Anal. Lett.* 33 (2000) 2293–2304.
- [30] P. Mukerjee, K. J. Mysels, *Critical Micelle Concentrations of Aqueous Surfactant Solutions*; National Bureau of Standards, (1970).
- [31] K. Kalyanasundaram, J.K. Thomas, Environment effects on vibronic band intensities in pyrene monomer fluorescence and their application in studies of micellar systems, *J. Am. Chem. Soc.* 99 (1977) 2039–2044.
- [32] R.M.M. Brito, W.L.C. Vaz, Determination of the critical micellar concentration of surfactants using fluorescent probe *N*-phenyl-1-naphthylamine, *Anal. Biochem.* 152 (1986) 250–255.
- [33] A. Mohr, P. Talbiersky, H.-G. Korth, R. Sustmann, R. Boese, D. Bläser, H. Rehage, A new pyrene-based fluorescent probe for the determination of critical micelle concentrations, *J. Phys. Chem. B* 111 (2007) 12985–12992.
- [34] D. Patra, C. Barakat, Unique role of ionic liquid [bmin][BF₄] during curcumin-surfactant association and micellization of cationic, anionic and non-ionic surfactant solutions, *Spectrochim. Acta Part A* 79 (2011) 1823–1828.
- [35] A. Kondoh, H. Yorimitsu, K. Oshima, Nucleophilic aromatic substitution reaction of nitroarenes with alkyl- or arylthio groups in dimethyl sulfoxide by means of cesium carbonate, *Tetrahedron* 62 (2006) 2357–2360.
- [36] A.H. Younes, T.H. Ghaddar, Synthesis and photophysical properties of ruthenium-based dendrimers and their use in dye sensitized solar cells, *Inorg. Chem.* 47 (2008) 3408–3414.
- [37] O. Maury, J.-P. Guégan, T. Renouard, A. Hilton, P. Dupau, N. Sandon, L. Toupet, H.L. Bozec, Design and synthesis of 4,4'-π-conjugated [2,2']-bipyridines: a versatile class of tunable chromophores and fluorophores, *New J. Chem.* 25 (2001) 1553–1566.
- [38] J.-P. Sauvage, J.-P. Collin, S. Chambron, C. Guillerez, V. Coudret, F. Balzani, L. De Cola, L. Fannigni, Ruthenium(II) and Osmium(II) bis(terpyridine) complexes in covalently-linked multicomponent systems: synthesis, electrochemical behaviour, absorption spectra, and photochemical and photophysical properties, *Chem. Rev.* 94 (94) (1994) 993–1019.
- [39] V. Balzani, S. Campagna, G. Denti, A. Juris, S. Serroni, M. Venturi, Designing dendrimers based on transition-metal complexes. Light-harvesting properties and predetermined redox patterns, *Acc. Chem. Res.* 31 (1998) 26–34.
- [40] K. Kalyanasundaram, Photophysics, photochemistry and solar energy conversion with tris(bipyridyl) ruthenium(II) and its analogues, *Coord. Chem. Rev.* 46 (1982) 159–244.
- [41] J.M. Lehn, Supramolecular chemistry-scope and perspective molecules supramolecular, and molecular devices, *Angew. Chem. Int. Ed.* 27 (1988) 89–112.
- [42] C.A. Slate, D.R. Striplin, J.A. Moss, P. Chen, B.W. Erickson, T.J. Meyer, Photochemical energy transduction in helical proline arrays, *J. Am. Chem. Soc.* 120 (1998) 4885–4886.
- [43] D.M. Klassen, G.A. Crosby, Spectroscopic studies of ruthenium(II) complexes. Assignment of the luminescence, *J. Chem. Phys.* 48 (1968) 1853–1858.
- [44] A.C. Bhasikuttam, M. Suzuli, S. Nakashima, T. Okada, Ultrafast fluorescence detection in tris(2,2'-bipyridine) ruthenium(II) complex in solution: relaxation dynamics involving higher excited states, *J. Am. Chem. Soc.* 124 (2002) 8398–8405.
- [45] M. Asha, Jhonsi, A. Kathiravan, G. Paramaguru, C. Manivannan, R. Renganathan, Fluorescence quenching of tri(2,2'-bipyridine) ruthenium(II) dichloride by certain organic dyes, *J. Solution Chem.* 39 (2010) 1520–1530.
- [46] A.A. Matí, J.L. Colón, Photophysical characterization of the interactions among tris(2,2'-bipyridyl) ruthenium(II) complexes ion-exchanged within zirconium phosphate, *Inorg. Chem.* 49 (2010) 7298–7303.
- [47] E. Kober, T.J. Meyer, Concerning the electronic structure of the ions M(bpy)₃³⁺ (MFe, Ru, Os: bpy_{2,2}-bipyridine), *Inorg. Chem.* 22 (1983) 1614–1616.
- [48] C. Dual, E.J. Baerends, P. Vemooijs, A density functional study of the MLCT states of [Ru(bpy)₃]²⁺ in D₃ symmetry, *Inorg. Chem.* 33 (1994) 3538–3543.
- [49] G.A. Crosby, W.H. Elfing Jr., Excited states of mixed ligand chelates of ruthenium(II) and rhodium(III), *J. Phys. Chem.* 80 (1976) 2206–2211.
- [50] F.E. Lytle, D.M. Hercules, Luminescence of tris(2,2'-bipyridine) ruthenium(II) dichloride, *J. Am. Chem. Soc.* 91 (1969) 253–257.
- [51] A. Juris, V. Balzani, F. Barigelletti, S. Campagna, P. Belser, A. von Zelewsky, Ru(II) polypyridine complexes: photophysics, photochemistry, electrochemistry and chemiluminescence, *Coord. Chem. Rev.* 84 (1988) 85–277.
- [52] J.V. Houten, R.J. Watts, The Effect of ligand and solvent deuteration on the excited state properties of the tris(2,2'-bipyridyl) ruthenium(II) Ion in aqueous solution. Evidence for electron transfer to solvent, *J. Am. Chem. Soc.* 97 (1975) 3843–3844.
- [53] T. Förster, G. Hoffmann, Effect of viscosity on the fluorescence quantum yield of a dye system, *Zeitschrift fuer Physikalische Chemie (Muenchen Germany)* 75 (1971) 63–76.
- [54] M. Bielawska, A. Chodźńska, B. Jańczuk, A. Zdziennicka, Determination of CTAB CMC mixed water + short-chain alcohol solvent by surface tension, conductivity, density and viscosity measurements, *Colloids Surf. A: Physicochem. Eng. Aspects* 424 (2013) 81–88.
- [55] Y. Shi, H.Q. Luo, N. Bing, Determination of the critical pre-micelle concentration first critical micelle concentration and second critical micelle concentration of surfactants by resonance Rayleigh scattering method without probe, *Spectrochim. Acta A* 78 (2011) 1403–1407.
- [56] N.C. Maiti, M.M.G. Krishna, P.J. Britto, N.J. Periasamy, Fluorescence dynamics of dye probes in micelles, *J. Phys. Chem. B* 101 (1997) 11051–11060.
- [57] J.M. Neugebauer, Detergents: an overview, *Meth. Enzymol.* 182 (1990) 239–253.
- [58] A. Fachini, I. Joekes, Interaction of sodium dodecyl benzene sulfonate with chrysotile fibers. Adsorption or catalysis? *Colloids Surf. A: Physicochem. Eng. Aspects* 201 (2002) 151–160.
- [59] K. Szymczyk, B. Jańczuk, The adsorption at solution-air interface and volumetric properties of mixtures of cationic and nonionic surfactant, *Colloids and Surf. A: Physicochem. Eng. Aspects* 293 (2007) 39–50.